applied sciences

MDPI

Article

Analysis of Transportation Hypernetwork Robustness Based on the Internal Structure of Hyperedges: A Case Study of China's High-Speed Railway

Bin Zhou [1,2], Xiujuan Ma [1,2,*] and Fuxiang Ma [1,2]

[1] School of Computer Science, Qinghai Normal University, Xining 810008, China; zhoub97@stu.qhnu.edu.cn (B.Z.); mfxmail@163.com (F.M.)
[2] The State Key Laboratory of Tibetan Intelligence, Qinghai Normal University, Xining 810008, China
* Correspondence: qhnumaxiujuan@163.com

Abstract

China's High-Speed Railway (HSR), the world's largest HSR system and a core component of national transportation, exhibits vulnerability in operational robustness to uncertain events such as natural disasters. Existing hypernetwork-based studies on HSR robustness often assume full connections among nodes within hyperedges, an assumption that deviates from reality. Using China's HSR line and station data, this paper constructs a real-world HSR hypernetwork and three reconstructed hypernetworks with distinct internal hyperedge structures. It also proposes a cascading failure model accounting for internal hyperedge structures and quantifies economic feasibility through an optimization cost index. Experimental results show the real-world HSR hypernetwork has scale-free properties. Sub-line density within hyperedges shows a positive correlation with robustness, where denser sub-lines enhance robustness. Prioritizing sub-line deployment around hub stations offers the most economical solution. This paper is the first to provide an HSR hypernetwork robustness optimization scheme from the perspective of internal hyperedge structures, offering theoretical reference for research on transportation networks with similar topological characteristics.

Keywords: high-speed railway hypernetwork; robustness; hyperedge internal structure; cascading failure

check for updates

Academic Editor: Suchao Xie

Received: 5 November 2025
Revised: 3 December 2025
Accepted: 5 December 2025
Published: 6 December 2025

Citation: Zhou, B.; Ma, X.; Ma, F. Analysis of Transportation Hypernetwork Robustness Based on the Internal Structure of Hyperedges: A Case Study of China's High-Speed Railway. *Appl. Sci.* **2025**, *15*, 12889. https://doi.org/10.3390/app152412889

Copyright: © 2025 by the authors. Licensee MDPI, Basel, Switzerland. This article is an open access article distributed under the terms and conditions of the Creative Commons Attribution (CC BY) license (https://creativecommons.org/licenses/by/4.0/).

1. Introduction

With the rapid development of the national economy, the demand for transportation systems is increasing. As the core backbone of China's 'Eight Vertical and Eight Horizontal' comprehensive transportation system, China's high-speed rail (HSR) has established the world's longest operating mileage (over 45,000 km as of 2024) and the widest-coverage HSR network [1–3]. However, the operational stability of HSR networks is vulnerable to impacts from various uncertain events, with severe consequences. According to public data from China State Railway Group Co., Ltd., outages during 2020–2024 were caused by extreme weather (over 60%), equipment failures (approximately 25%), and geological hazards (15%). Typical examples include: extreme rainstorms in Henan in 2021 caused line paralysis around Zhengzhou East Railway Station, affecting over 100,000 passengers in a single day. Typhoon Yagi in 2023 led to the suspension of 134 trains operated by Guangzhou Railway Group, with refund and emergency response costs exceeding 30 million yuan. The 2022 Luding earthquake in Sichuan caused tunnel damage to the Chengdu-Ya'an HSR,

resulting in 72 h of suspended operation. These events highlight the urgent need to improve HSR network robustness, which ensures the safety of national transportation lifelines and supports sustainable economic and social development.

For the analysis of transportation network robustness, researchers have developed multiple technical approaches. On the one hand, studies based on complex network theory have achieved abundant results: Lordan and Sallan [4] investigate the robustness of European airport networks based on k-core decomposition, revealing the impact of multi-layered structures; Du et al. [5] analyze China's air transport network and find that robustness is optimal when low-degree nodes are removed; Zhang et al. [6] focus on high-speed rail networks in China, the United States, and Japan, proposing a neighbor link intervention method to improve reliability; Wandelt et al. [7] leverage community structures to enhance the efficiency of robustness analysis for large-scale transportation networks; Hu et al. [8] integrate passenger flow data to construct a high-speed rail network model and identify key corridors; and Mei et al. [9] evaluate the disaster resilience of multi-layer coupled transportation networks. On the other hand, artificial intelligence (AI) methods have gradually become an important supplement to transportation reliability assessment [10,11] in recent years: Li et al. [12] propose a heterogeneous graph neural network (HetGNN) model to analyze train delay evolution in railway networks, capturing interactions between different entities to assess the network's robustness against disturbances; Liu et al. [13] adopt an AI-driven passenger flow assignment and performance evaluation model, quantifying the performance loss of subway stations and systematically evaluating their robustness levels under various disturbance scenarios such as sudden passenger flow surges and equipment failures; Xia et al. [14] establish a machine learning framework to analyze the robustness of China's railway network, finding weak robustness through node attack simulations and clarifying the need to strengthen cross-regional connections to improve the network's disturbance resistance capability.

Overall, existing studies primarily rely on graph theory models (e.g., node-edge topology) [15,16]. However, these graphs fail to depict complex relationships, such as one-to-many and many-to-many. Hypernetwork theory directly expresses collaborative relationships among multiple nodes through hyperedges [17–20], providing a more practical tool for modeling transportation systems such as high-speed rail. It has gradually become a research hotspot in recent years. However, existing hypernetwork-based transportation studies still have obvious limitations. First, the assumption of full connectivity among nodes within a hyperedge is disconnected from reality. Most studies assume full connectivity among all nodes within a hyperedge to simplify calculations. For example, Wei et al. [21] adopt this assumption when constructing the Nanjing subway hypernetwork. Luo et al. [22] use it when analyzing urban public transport hypernetworks. Tang et al. [23] and Yin et al. [24] also apply it when studying high-speed rail hypernetworks. But in real high-speed rail networks, stations only maintain physical connections with adjacent stations. The full connectivity assumption causes significant deviations between the model and actual physical logic. Second, cascading failure models regard hyperedges as "black boxes". Existing models mostly ignore the constraints of the internal connection mode of hyperedges on load redistribution paths. For instance, the hypernetwork cascading model proposed by Chen et al. [25] only distributes load based on the number of hyperedges. It does not consider the actual connectivity relationships between nodes within hyperedges. It is difficult to accurately simulate the load transfer process after failures. Third, existing optimization schemes fail to quantify the construction costs for robustness improvement. Existing optimization schemes mostly focus on the single objective of improving robustness. For example, Ma et al. [26] study the role of capacity expansion in improving resilience but do not calculate the expansion costs. In practical engineering, measures such as new

sub-line construction and hub reconstruction require substantial funds. Ignoring costs makes it difficult for schemes to be implemented.

Consequently, these limitations make existing hypernetwork-based studies struggle to effectively support optimal decision-making for the systematic operation of transportation networks. For example, such studies fail to address how to balance robustness and costs through specific strategies like prioritizing sub-line deployment. There is an urgent need to construct an accurate cascading failure model that better aligns with real-world topologies. An optimization strategy balancing performance and economics should be proposed to assess economic feasibility. Such a strategy aims to achieve the optimal robustness-cost trade-off.

Existing studies have not overcome the hyperedge black-box assumption or established a robustness-cost collaborative evaluation framework. Additionally, they lack targeted analysis of various unexpected event scenarios. To address these gaps, this study takes China's high-speed rail as a case study. It focuses on the impact of internal hyperedge structures on the robustness of high-speed rail hypernetworks. The main contributions of this paper are reflected in the following three aspects:

- Based on data of China's high-speed railway, a realistic hypernetwork is constructed for the first time where nodes within hyperedges only maintain adjacent connections (denoted as HSR-A hypernetwork). Three reconstructed hypernetworks are also specifically designed: HSR-R hypernetwork (nodes within hyperedges are randomly connected), HSR-P hypernetwork (nodes within hyperedges are preferentially connected), and HSR-F hypernetwork (nodes within hyperedges are fully connected). This provides a complete model foundation for analyzing the relationship between the internal structure of hyperedges and robustness.
- Based on the capacity-load model, this study improves the load distribution mechanism and proposes a cascading failure model more suitable for hypernetwork structures. It solves the problem that existing models ignore internal hyperedge structures and improves the accuracy of cascading failure analysis.
- An optimization cost index is defined to quantitatively evaluate the economy of different hypernetworks. It finds that the HSR-P hypernetwork can ensure robustness while significantly reducing construction costs and avoiding sub-line redundancy, providing an implementable optimization strategy for engineering practice.

The remainder of this paper is structured as follows. Section 2 describes the mathematical definition of hypernetworks. It also presents a cascading failure model that accounts for the internal structure of hyperedges. Section 3 introduces the data processing workflow of China's high-speed railway. It details the construction steps of the four hypernetworks (HSR-A/R/P/C hypernetwork). It also analyzes their topological characteristics. Section 4 presents the robustness of the four hypernetworks under random attacks and deliberate attacks. Section 5 quantifies the economy of different hypernetworks based on the optimization cost index. It also proposes optimization strategies. Section 6 summarizes the research conclusions.

2. Model Description and Definitions

2.1. Hypernetwork Definition

The definition of a hypergraph first proposed by Berge [17,18] states the following: if a binary relation $H = (V, E)$ satisfies the condition: $\emptyset \neq e_i \in P(V), i \in \{1, 2, \cdots, m\}$, then H is called a hypergraph. Here, $V = v_1, v_2, \ldots, v_n$ and $E = e_1, e_2, \ldots, e_m$, while $P(V)$ denotes the power set of set V. Elements in set V are called nodes of the hypergraph. Elements in E are called hyperedges of the hypergraph. If the nodes within a hyperedge e_i are not

contained in any other hyperedge, then this hyperedge is called an isolated hyperedge. The number of nodes $|V| = N$ of hypergraph is called the order of hypergraph H. Similarly, the number of hyperedges $|E| = M$ is called the size of hypergraph H. The rank of hypergraph H refers to the maximum number of nodes contained in a hyperedge, denoted as $r(H) = \max_i |e_i|, (i = 1, 2, \ldots, M)$. In contrast, the co-rank of hypergraph H refers to the minimum number of nodes contained in a hyperedge, denoted as $cr(H) = \min_i |e_i|, (i = 1, 2, \ldots, M)$. If $r(H) = cr(H) = k$, then hypergraph H is called a k-uniform hypergraph or simply a uniform hypergraph. Otherwise, hypergraph H is a non-uniform hypergraph.

Hypernetwork is a network formed by abstracting complex systems with hypergraph as the topological structure. Here, k can represent the scale of uniform hypernetworks, and $r(H)$ can represent the scale of non-uniform hypernetworks. Moreover, hypernetworks effectively express a certain relationship that multiple nodes satisfy simultaneously through hyperedges. They are more intuitive than networks based on ordinary graphs. For instance, an author collaboration hypernetwork expresses the scenario where multiple authors cooperate on the same paper. A transportation hypernetwork expresses the scenario where multiple transportation stations are passed by the same transportation line. In a hypernetwork, the hyperdegree of a node v_i is defined as the number of hyperedges containing node v_i, denoted as $d_H(v_i)$. In contrast, the node degree of node v_i, similar to that in ordinary networks, is still defined as the number of ordinary edges associated with node v_i, denoted as $d(v_i)$. The intra-hyperedge node degree of node v_i within a single hyperedge e_i is denoted as $k_{e_i}(v_i)$. Figure 1 shows a hypergraph satisfying the binary relation $H = (V, E)$. This hypergraph has a total of 5 hyperedges and 11 nodes. For example, taking node v_2: its hyperdegree $d_H(v_2)$ is 3, its node degree $d(v_2)$ is 5, and its intra-hyperedge node degrees $k_{e_i}(v_2)$ within hyperedges e_1, e_2, and e_3 are 1, 2, and 2, respectively.

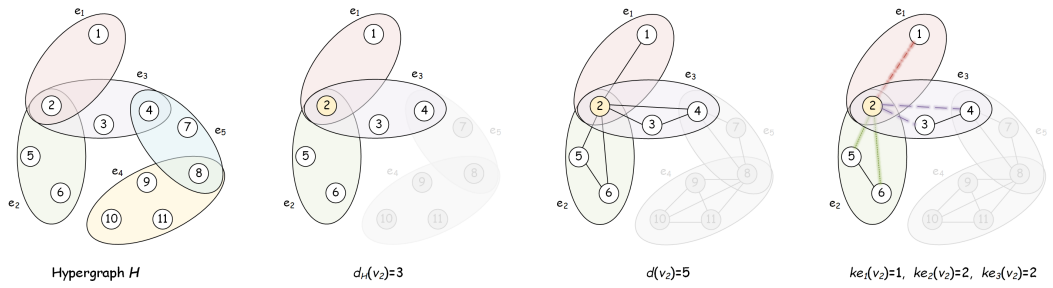


Figure 1. Schematic of Hypergraph and Topological Quantities.

2.2. Hypernetwork Cascading Model Based on Intra-Hyperedge Structure

The hypernetwork cascading failure model proposed by previous researchers [25] has the problem of overly single considered indicators. It often converts hypernetworks into line graphs for research. This ignores the impact of the interaction between node connections within hyperedges. To better describe the impact of the internal structure of hyperedges on hypernetwork robustness, a new cascading failure model is proposed based on the capacity-load model [27]. It is used to analyze the relationship between the internal structure of hyperedges and hypernetwork robustness.

In a hypernetwork with N nodes, the initial load of node v_i is related to its hyperdegree $d_H(v_i)$ and node degree $d(v_i)$. Its initial load, denoted as $L_{v_i}(0)$, is defined as follows:

$$L_{v_i}(0) = \alpha(d_H(v_i) + d(v_i))^{\beta} \quad i = 1, 2, \cdots, N, \alpha \geqslant 1, \beta \geqslant 1, \tag{1}$$

To control the initial load of node v_i, let α be the load parameter and β be the adjustable parameter. Specifically, α is used to control the overall magnitude of the initial load of

nodes. The default value of α is $\geqslant$1 to simulate scenarios with different load intensities. β is used to adjust the nonlinear relationship between load and node degree (hyperdegree + ordinary degree). The default value of β is $\geqslant$ 1. When $\beta \geqslant 1$, it emphasizes the load amplification effect of high-degree nodes. This makes the model more consistent with the actual load distribution of transportation hubs. If node v_i fails, its load is distributed to its non-failed neighbor node v_j in the following two steps.

Step 1: First, it is allocated to the associated non-failed hyperedges according to the priority probability $\prod_{hyper-edge}$.

$$\prod_{hyper-edge} = \frac{|e_i|}{\sum_{e_m \in E_{v_i}} |e_m|}, \tag{2}$$

where E_{v_i} denotes the set of all associated non-failed hyperedges of the failed node v_i. $|e_i|$ denotes the number of nodes contained in hyperedge e_i. For example, in an express delivery service hypernetwork, $|e_i|$ is the number of express delivery stations included in the delivery area.

Step 2: After the failed node vi distributes its own load to the adjacent non-failed hyperedges according to Equation (2), the load allocated to the hyperedges is further distributed to the associated non-failed nodes of v_i within hyperedge e_i based on the priority probability $\prod_{node}$. For example, in an express delivery service hypernetwork, $k_{e_i}(v_i)$ refers to the number of adjacent non-failed stations of the failed station within the same delivery area.

$$\prod_{node} = \frac{k_{e_i}(v_i)}{\sum_{v_r \in \Gamma_{v_i}} k_{e_i}(v_r)}, \tag{3}$$

where Γ_{v_i} denotes the set of all non-failed neighbor nodes of the failed node v_i within hyperedge e_i. The load received by node vj is as shown in Equation (4).

$$\Delta L_{v_i \to v_j} = L_{v_i} \times \Pi_{hyper-edge} \times \Pi_{node}. \tag{4}$$

It can be seen from Equation (4) that the additional load $L_{v_i \to v_j}$ received by node v_j within hyperedge e_i is related to three factors. These factors are the number of associated nodes in the hyperedge it belongs to, the ordinary degree of node v_j within hyperedge e_i, and the initial load of node v_i.

In a hypernetwork, the capacity of a node is the maximum load it can handle. It is proportional to the node's initial load. Let the capacity of node v_j be denoted as C_{v_j}. It is expressed by Equation (5):

$$C_{v_j} = (1 + T)L_{v_j} \quad T \geqslant 0, \tag{5}$$

where T is the capacity parameter. The larger the value of T, the larger the node's capacity. The stronger its ability to resist failures, but the higher the resistance cost. The critical threshold T_C is the minimum capacity value to avoid global collapse of the hypernetwork. When $T > T_C$, the entire hypernetwork will not experience global collapse. When $T < T_C$, the entire hypernetwork will undergo global collapse. Thus, the critical threshold T_C of T is an important indicator for measuring hypernetwork robustness. Obviously, the smaller the T_C, the more robust the hypernetwork.

If node v_j fails after receiving the additional load, it satisfies the following inequality:

$$L_{v_j} + L_{v_i} \times \frac{|e_i|}{\sum_{e_m \in E_{v_i}} |e_m|} \times \frac{k_{e_i}(v_j)}{\sum_{v_r \in \Gamma_{v_i}} k_{e_i}(v_r)} > C_{v_j}. \tag{6}$$

If Equation (6) holds, node v_j overloads and fails. After the load of v_j is redistributed, it may cause other nodes to fail.

To measure the robustness of a hypernetwork, initially attack node vi and make it fail. Then redistribute its load. For other nodes after load redistribution, if they satisfy Equation (7), they fail. When all nodes within a hyperedge fail, the hyperedge fails. Once the number of failed nodes in the hypernetwork reaches a stable state or all nodes fail (global collapse), count the number of failed hyperedges $F_M(0 \leqslant F_M \leqslant M)$. Calculate the failed hyperedge ratio f_M as shown in Equation (7):

$$f_M = \frac{F_M}{M} \quad 0 \leqslant f_M \leqslant 1, \tag{7}$$

where M is the total number of hyperedges in the hypernetwork. It can be seen from Equation (7) that the larger f_M is, the more failed hyperedges there are in the hypernetwork. This means the poorer the robustness of the hypernetwork.

3. Construction of Hypernetwork Model

3.1. Datasets

The China's high-speed railway dataset used in this paper is derived from the China HSR Network. Data processing yields 119 lines and 1195 stations. Among these, the high-speed rail (HSR) in Hainan Province is a loop line. This line has no intersections with other lines in the HSR network. It functions as an independent hyperedge. If retained, its isolated nature interferes with the calculation of the robustness critical threshold T_C. This interference results in the inability to accurately determine T_C. To facilitate the identification of the robustness critical threshold of the HSR hypernetwork, the Hainan loop line is excluded when constructing the HSR hypernetwork. Further data processing results in a final dataset with 118 lines and 1169 stations. The distribution map of stations included in each line of China's HSR network is shown in Figure 2. It can be clearly observed from the map that the number of stations included in each line of China's HSR network varies. This aligns with the characteristics of non-uniformity. Specifically, a single line has a minimum of 2 stations and a maximum of 55 stations. Thus, China's HSR network is suitable for modeling with a non-uniform hypernetwork.

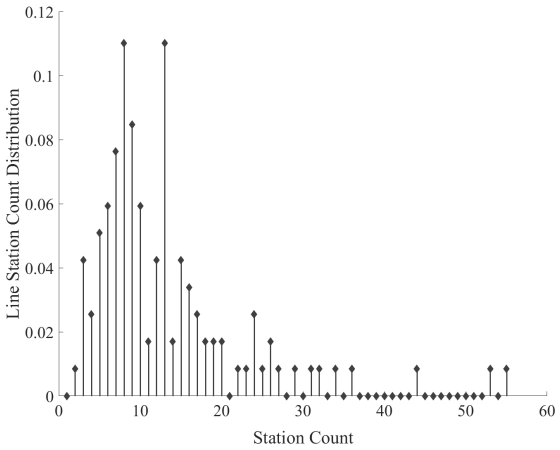


Figure 2. Distribution of Lines and Stations in China's HSR Network.

3.2. Modeling of China's HSR Hypernetwork

In this section, the 118 processed lines in China's HSR network are abstracted as hyperedges in the hypernetwork. The 1169 stations are abstracted as nodes. In the HSR hypernetwork, $M = 118$, $N = 1169$, and $r(H) = 55$. To focus the analysis on the impact of the inter-station structure within lines on its robustness, several factors are not considered. These factors include line overlap, line transport capacity, and the operation direction

of high-speed railways. The finally constructed HSR hypernetwork is an undirected, unweighted, and non-uniform hypernetwork.

First, number the collected station and line data. Use numbers to represent the corresponding nodes and hyperedges, and store the numbered station and line data in an Excel spreadsheet. Define the incidence matrix of China's HSR hypernetwork. Use MATLAB R2017a to read the data in Excel. Store the data in the incidence matrix with rows corresponding to lines and columns corresponding to stations. This constructs an incidence matrix of 118 rows and 1169 columns. To better describe the connection relationship between stations within lines in the real HSR network, the internal structure of lines conforms to the actual adjacency relationship of stations. The constructed HSR hypernetwork is denoted as the HSR-A hypernetwork. The detailed construction method is shown in Algorithm 1.

Algorithm 1 Construction of HSR Hyper-Network

Input: $hyperedge_index \in N^{M \times r(H)}$, $M = 118$, $r(H) = 55$, $N = 1169$;
Output: $HSR_{hyper_adjmatrix} \in \{0,1\}^{N \times N}$

Initialize $HSR_{hyper_adjmatrix}$ as an $N \times N$ zero matrix
for each hyper-edge i from 1 to M **do**
  for each node index j from 1 to $r(H) - 1$ **do**
    if $hyperedge_index[i,\ j+1] \neq 0$ (i.e., the next node in the hyper-edge exists) **then**
      $HSR_{hyper_adjmatrix}[hyperedge_index[i,j], hyperedge_index[i,j+1]] = 1$
      $HSR_{hyper_adjmatrix}[hyperedge_index[i,j+1], hyperedge_index[i,j]] = 1$
    else
      break the inner loop(end of nodes in current hyperedge)
    end if
  end for
end for
return $HSR_{hyper_adjmatrix}$

3.3. China's HSR Hypernetwork Construction Based on Hyperedge Internal Structure

To better explore the impact of internal hyperedge structures on hypernetwork robustness, this study builds three high-speed rail (HSR) hypernetworks (HSR-R, HSR-P, HSR-F). The construction is based on the HSR-A hypernetwork's design concept and integrates different internal hyperedge connection modes. The core classification criterion lies in the internal connection logic of hyperedges, with specific designs and functions as follows: Specifically, HSR-R adopts a random connection mode. It takes the random complex network model as a benchmark. It is used to compare the impact of unbiased deployment on the hypernetwork. Its connection logic is similar to the unplanned addition of temporary sub-lines. HSR-P adopts a preferential attachment mode. It is constructed based on the Barabási-Albert model. It is used to simulate the preferential growth characteristics of high-hyperdegree hub nodes. This mode is similar to prioritizing the deployment of backup lines around hub stations. HSR-F adopts a fully connected mode. It serves as an ideal performance benchmark. It is used to evaluate the hypernetwork performance corresponding to the upper limit of hyperedge density. Its design is similar to the ideal form of a high-density urban rail network and is relatively rare in practical applications. The specific construction processes of the three hypernetworks are as follows.

Step 1: Construct the HSR hypernetwork; see Algorithm 1 for details.

Step 2: Disconnect the original connections between nodes within the hyperedge. When a random connection method is adopted between nodes within the hyperedge (this method refers to randomly reconnecting node pairs within the hyperedge with a probability

$p \in [0,1]$, and is used to simulate unbiased random sub-line deployment), proceed to (1). When a preferential attachment method is adopted (this method refers to prioritizing the reconnection of high-hyperdegree nodes, and is used to simulate the real-world hub-prioritized connection mode; here, δ_m serves as the parameter for preferential attachment, representing the selection of k nodes with the highest hyperdegree from the hyperedge H for connection—to quantify the degree of preference and avoid excessive computational complexity), proceed to (2). When a fully connected method is adopted, proceed to (3).

1. HSR-R hypernetwork:
   (a) Initialization: Make the $k(1 \leq k \leq N)$ nodes within hyperedge $e_i(1 \leq i \leq M)$ become isolated nodes in the induced subgraph $G(e_i)$ of hyperedge e_i. Assign the probability $p \in [0,1]$ of node reconnection;
   (b) Nodes within the hyperedge reconnect randomly in the following way: First, generate a random number r. Then, randomly select a pair of nodes within the same hyperedge. If $r < p$, check whether there is an edge between the selected node pair. If there is no edge, connect them with an ordinary edge; otherwise, do nothing.
   (c) Repeat Step (b) until $p \times k(k-1)/2$ ordinary edges are generated.
2. HSR-P hypernetwork:
   (a) Initialization: Let V_{e_i} denote the node set within hyperedge e_i. The $k(1 \leq k \leq N)$ nodes in $e_i(1 \leq i \leq M)$ serve as isolated nodes in the induced subgraph $G(e_i)$ of hyperedge e_i. Select 3 nodes and make them fully connected to form the initial connected component C_0 within the hyperedge. Let Γ_t denote the node set of the connected component C_t within the hyperedge at time t;
   (b) Growth: At time $t+1$, randomly select a node $v_k(v_k \in V_{e_i}, v_k \notin C_t)$ outside the connected component C_t. Add it to C_t to form the new connected component C_{t+1}. When v_k joins the connected component, select a node $v_i(v_i \in V_{e_i}, v_i \in C_t)$ within C_t in the manner described in (c). Repeat Step (b) to continuously expand the connected component until it includes all nodes in hyperedge e_i.
   (c) Preferential attachment: Let $k_{e_i,C_t}(v_i)$ denote the ordinary degree of node v_i within hyperedge e_i in the connected component C_t. Node v_k outside the connected component C_t selects δ_m nodes within the component and connects with them via ordinary edges. Node v_i within the component is selected with the preferential attachment probability $\prod_i$.

$$\prod_i = \frac{k_{e_i}(v_i)}{\sum_{j=1}^{|\Gamma_t|} k_{e_i}(v_j)}, \quad v_i, v_j \in C_t. \tag{8}$$

3. HSR-F hypernetwork:
   (a) Initialization: Make the $k(1 \leq k \leq N)$ nodes within hyperedge $e_i(1 \leq i \leq M)$ become isolated nodes in the induced subgraph $G(e_i)$ of hyperedge e_i.
   (b) Node reconnection within the hyperedge: For the k nodes, connect each pair of distinct nodes with exactly one ordinary edge. This generates a complete connected subgraph that contains k nodes and $k(k-1)/2$ edges.

Step 3: Repeat Step 2 until all hyperedges in the hypernetwork are traversed.

3.4. Analysis of Topological Characteristics

Node degree and node hyperdegree are important indicators reflecting the hypernetwork structure. In this section, the analysis focuses on the node degrees and their degree distributions of the HSR-A hypernetwork, HSR-R hypernetwork, HSR-P hypernetwork, and HSR-F hypernetwork.

3.4.1. Node Hyperdegree Distribution

Node hyperdegree is one of the indicators for measuring node importance in hypernetworks. In the HSR hypernetwork, node hyperdegree refers to the number of HSR lines passing through a station. Table 1 presents the top 10 stations with the highest node hyperdegrees in the HSR hypernetwork. It can be observed from the table that these top 10 stations are mostly provincial capitals or transportation hub cities. Figure 3 shows the node hyperdegree distribution of the HSR hypernetwork. It can be observed that the node hyperdegree distribution follows a power-law distribution. This indicates that the HSR hypernetwork has scale-free properties. Specifically, fewer stations are traversed by multiple lines, while most stations are traversed by only a few lines. Such a characteristic reflects the actual situation of China's HSR network. To verify the rationality of the assumption that node hyperdegree distribution conforms to a power-law, statistical analysis was conducted on the node hyperdegree $d_H(v_i)$ of the HSR-A hypernetwork using power-law fitting $P(k) \sim k^{-\gamma}$. The fitting results showed that the power-law exponent γ = 3.98 and the goodness of fit R^2 = 0.92. This value means the model explains 92% of the variance changes. Further, a Kolmogorov-Smirnov (KS) test was performed. The KS statistic is 0.05, with a p-value of 0.42 (>0.05). This result indicates that the null hypothesis of power-law distribution cannot be rejected. In comparison with comparative values (e.g., the fitting of random Poisson networks yields an R^2 of only 0.91 and a KS p-value of 0, which rejects the power-law hypothesis), the power-law fitting in this study is significantly better. This confirms the scale-free property of the HSR network, which is consistent with the hub-and-spoke layout of China's HSR.

Table 1. Top 10 Stations by Node Hyperdegree in the HSR Hypernetwork.

Rank	Node ID	Station	Hyperdegree Value
1	114	Chengdu East	7
2	391	Beijing West	7
3	253	Shanghai Hongqiao	6
4	53	Xi'an North	5
5	63	Zhengzhou East	5
6	72	Xuzhou East	5
7	394	Beijing South	5
8	244	Hangzhou East	5
9	163	Guiyang North	5
10	35	Lanzhou West	5

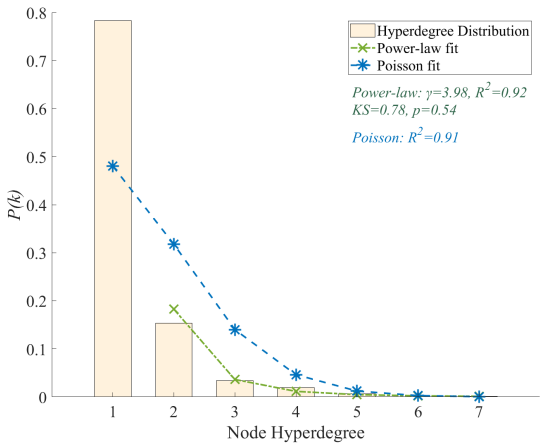


Figure 3. Node Hyperdegree Distribution of the HSR Hypernetwork.

3.4.2. Node Degree Distribution

Node degree is another important indicator for measuring node importance. It is also one of the key metrics for evaluating the significance of a station in the HSR hypernetwork. Node degree reflects a station's influence and connection level in the HSR hypernetwork. A higher node degree value of a station indicates greater influence and a higher connection level in the hypernetwork. It also plays an important role in the transportation efficiency and stability of the HSR hypernetwork. Below are the top 10 stations by node degree in the HSR-A, HSR-R, HSR-P, and HSR-F hypernetworks. Also presented are the node degree distributions of the HSR hypernetworks with three different internal hyperedge structures.

Table 2 presents the top 10 stations by node degree in the HSR-A hypernetwork. It can be observed that the HSR-A hypernetwork has relatively small node degree values. This is due to the limitation of its internal hyperedge structure—nodes in the hypernetwork have fewer one-hop neighbors. The station with the highest node degree is Zhengzhou East Railway Station, with a node degree value of 7. Figure 4a shows the node degree distribution of the HSR-A hypernetwork.It can be seen from the figure that approximately 80% of the nodes have a degree value of 2, meaning each such node has 2 one-hop neighbors. This is because, in the HSR hypernetwork, a station on the same line is usually directly connected to two adjacent stations. Thus, stations with a node degree of 2 account for the majority.Among these nodes, the minimum node degree value is 1. This indicates the station is directly adjacent to only one other station, such as Yining Railway Station.

Table 2. Top 10 Stations by Node Degree in the HSR-A Hypernetwork.

Rank	Node ID	Station	Degree Value
1	63	Zhengzhou East	7
2	53	Xi'an North	7
3	253	Shanghai Hongqiao	6
4	72	Xuzhou East	5
5	391	Beijing West	5
6	278	Wuhan	5
7	523	Guangzhou South	5
8	88	Chongqing North	5
9	163	Guiyang North	5
10	35	Lanzhou West	5

Table 3 presents the top 10 stations by node degree in the HSR-R hypernetwork. It can be observed that Hangzhou East Railway Station has the highest node degree. This means the station has the most accessible stations and strong hub capacity. Meanwhile, combined with the degree distribution in Figure 4b, a key finding emerges. Stations within the lines adopt a random connection method. Thus, the HSR-R hypernetwork's node degree distribution exhibits a Poisson-then-power-law characteristic. Additionally, the node degree values of the top 10 stations are relatively uniform. This indicates that these stations are all important hub stations. The top 10 stations connect a large number of other stations and maintain numerous interconnections. This also aligns with the actual situation of real-world stations. Stations such as Chengdu East Railway Station and Xi'an North Railway Station are highly important hub nodes. Such a uniform distribution shows that the hub stations of the HSR-R hypernetwork are reasonably distributed. Reasonable hub station distribution effectively enables the circulation of information and passengers.

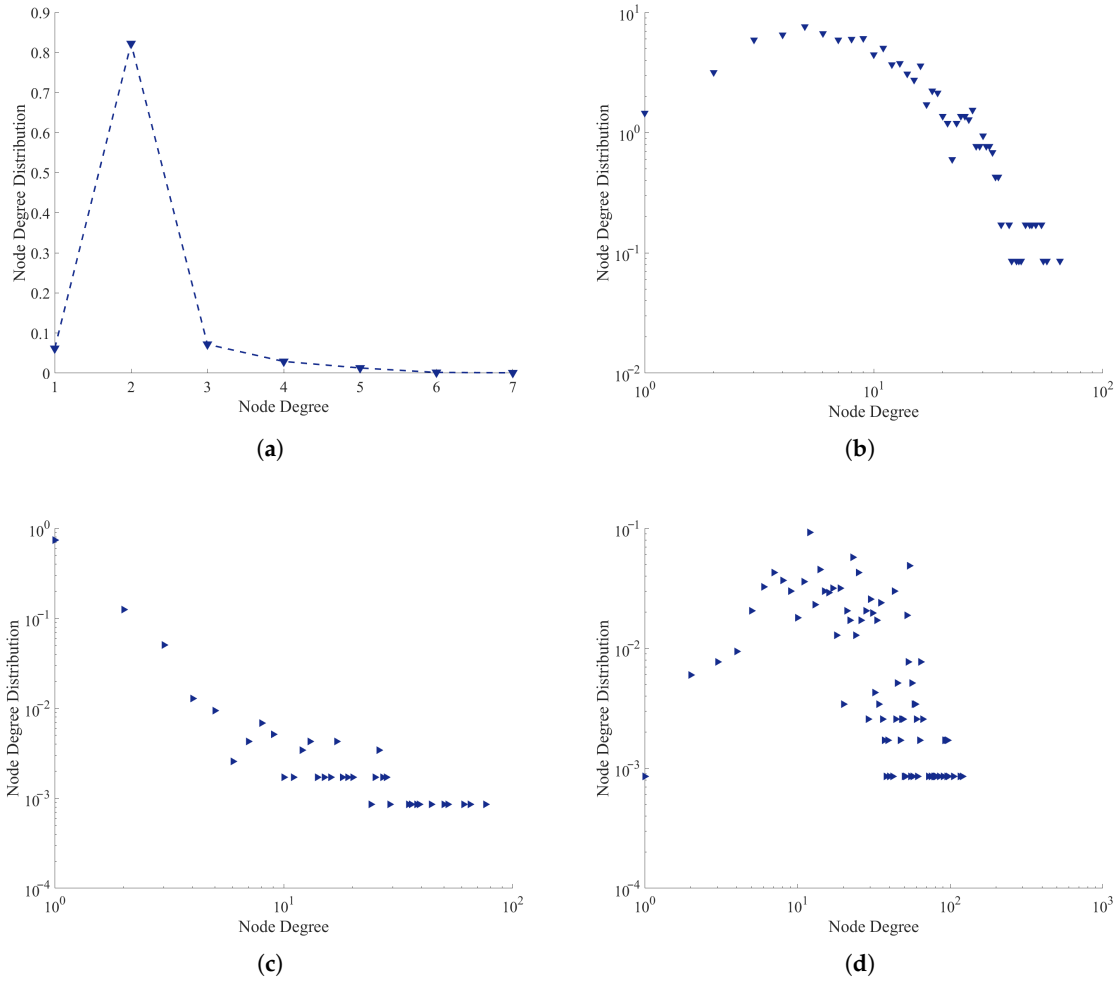


Figure 4. Node Degree Distributions of HSR Hypernetworks: (**a**) HSR-A hypernetwork; (**b**) HSR-R hypernetwork; (**c**) HSR-P hypernetwork; (**d**) HSR-F hypernetwork.

Table 3. Top 10 Stations by Node Degree in the HSR-R Hypernetwork.

Rank	Node ID	Station	Degree Value
1	244	Hangzhou East	65
2	114	Chengdu East	57
3	53	Xi'an North	55
4	193	Kunming South	54
5	253	Shanghai Hongqiao	54
6	163	Guiyang North	51
7	523	Guangzhou South	51
8	278	Wuhan	49
9	527	Shenzhen North	49
10	225	Changsha South	48

Table 4 presents the top 10 stations by node degree in the HSR-P hypernetwork. It can be observed that under this internal hyperedge node connection method, Xi'an North Railway Station has the highest node degree. The station also boasts strong hub capacity. Among the top 10 stations, the node degree difference between Xi'an North Railway Station (ranked 1st) and Chongqing North Railway Station (ranked 10th) reaches 41. The node

degree gap between Xi'an North Railway Station and other stations is also very significant. The minimum degree difference stands at 11. This indicates that Xi'an North Railway Station has extremely strong connectivity in the entire hypernetwork. Chongqing North Railway Station, in contrast, has relatively weak connectivity. This also aligns with real-world conditions. The discrepancy relates to the geographical locations and traffic volumes of the two stations. As an important railway hub in Shaanxi Province, Xi'an North Railway Station connects multiple railway lines. The station has a high node hyperdegree value and large traffic volume. Thus, its node degree value is also high. Chongqing North Railway Station, while also an important railway hub, is geographically more remote compared to Xi'an North Railway Station. The surrounding transportation network of Chongqing North Railway Station is relatively weak. Therefore, its node degree value is lower. Figure 4c shows the node degree distribution of the HSR-P hypernetwork. It can be seen from the figure that the node degree distribution exhibits the fat-tail characteristic of a power-law distribution. This means that in the HSR-P hypernetwork, a small number of nodes have extremely high degrees. Most nodes, however, have relatively low degrees.

Table 4. Top 10 Stations by Node Degree in the HSR-P Hypernetwork.

Rank	Node ID	Station	Degree Value
1	53	Xi'an North	76
2	244	Hangzhou East	65
3	163	Guiyang North	61
4	63	Zhengzhou East	52
5	421	Shenyang North	50
6	391	Beijing West	44
7	193	Kunming South	39
8	35	Lanzhou West	38
9	72	Xuzhou East	36
10	88	Chongqing North	35

Under the full connection method of internal hyperedge nodes in the HSR-F hypernetwork, the top 10 stations by node degree are presented in Table 5. Among these stations, Hangzhou East Railway Station has the highest node degree, with a value of 120. The HSR-F hypernetwork adopts a full connection method for internal hyperedge nodes. Each node connects directly to all other nodes. Thus, node degree values in the HSR-F hypernetwork are relatively large. In contrast, the HSR-A, HSR-R, and HSR-P hypernetworks have relatively small node degree values. The difference stems from the distinct connection methods between nodes in these three hypernetworks. Figure 4d shows the node degree distribution of the HSR-F hypernetwork. It can be seen from the figure that the node degree distribution still exhibits obvious fat-tail characteristics. However, the continuity of the degree distribution is poor. The cause of this degree distribution is related to the number of stations in HSR lines. When the full connection method is adopted, the node degree of each station is improved. For some HSR stations that have more passing lines and are located in lines with a larger number of stations, the node degree improvement is more significant due to this connection method.

Table 5. Top 10 Stations by Node Degree in the HSR-F Hypernetwork.

Rank	Node ID	Station	Degree Value
1	244	Hangzhou East	120
2	523	Guangzhou South	116
3	391	Beijing West	105
4	527	Shenzhen North	97
5	63	Zhengzhou East	96
6	193	Kunming South	96
7	225	Changsha South	95
8	253	Shanghai Hongqiao	94
9	278	Wuhan	94
10	163	Guiyang North	92

4. Trial and Applications

In this section, the hypernetwork cascading failure model based on internal hyperedge structure is applied to the HSR-A hypernetwork and the three HSR hypernetworks with different internal hyperedge structures. The robustness of the HSR-A, HSR-R, HSR-P, and HSR-F hypernetworks under random attacks and deliberate attacks is obtained. The influence of internal hyperedge structure on the robustness of HSR hypernetworks is analyzed and derived.

4.1. Parameter Sensitivity Analysis

To eliminate the impact of other uncertain factors on the robustness of HSR hypernetworks, a parameter sensitivity analysis is conducted here, as shown in Figure 5. It can be observed from Figure 5a that all three HSR hypernetworks are relatively sensitive to parameter α. As the value of parameter α increases, the critical threshold T_C shows a fluctuating trend. Among them, the HSR-P hypernetwork exhibits the most significant fluctuation with changes in parameter α, with a maximum fluctuation of 0.12. The HSR-F hypernetwork has the smallest fluctuation (0.05) with parameter α. The curve fluctuations also indicate that the HSR-F hypernetwork shows relatively stronger stability against changes in parameter α. This is attributed to its greater number of ordinary edges $m_{|e_i|}$. When α equals 10, the three HSR hypernetworks achieve optimal robustness. As shown in Figure 5b, the robustness critical threshold T_C of all three HSR hypernetworks presents an exponential growth trend with parameter β. The HSR-P hypernetwork is the most sensitive to parameter β, exhibiting the largest increase in its critical threshold as β increases. In brief, the robustness of the three HSR hypernetworks degrades as parameter β increases. When β equals 1, the three HSR hypernetworks reach their optimal robustness.

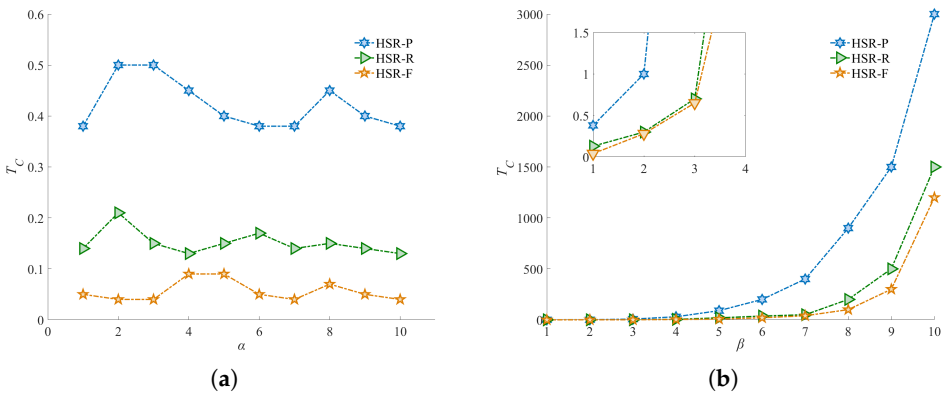


Figure 5. The Impact of Parameters α and β on the Robustness of Three HSR Hypernetworks: (**a**) Parameters α; (**b**) Parameters β.

4.2. Attack Strategy

Random attack refers to randomly selecting a node in the hypernetwork for attack. In contrast, deliberate attack involves selecting the most important node in the hypernetwork for attack. Since this study focuses on the impact of internal hypernetwork structures on robustness, due to the particularity of hypernetwork structures, the index under the combined effect of intra-hyperedge and inter-hyperedge structures is adopted when selecting the most important node in the hypernetwork. This indicator is denoted as: comprehensive importance of hypernetwork nodes. It is shown in Equation (9). The comprehensive importance indicator of hypernetworks essentially selects the node with the maximum sum of the proportion of node degree value and the proportion of node hyperdegree value in the hypernetwork. After a node fails due to attack, the load of the failed node is evenly distributed to its adjacent non-failed nodes. To ensure the validity of the experiment, experimental results take the average value of 50 independent runs.

$$S_i = \max_i \left| \frac{d(v_i)}{\sum_i d(v_i)} \right| + \max_i \left| \frac{d_H(v_i)}{\sum_i d_H(v_i)} \right|, \quad i = 1, 2, \cdots, N. \tag{9}$$

4.3. Robustness Analysis

Figure 6 shows the variation in the hyperedge failure ratio f_M with the capacity parameter T when the HSR-A hypernetwork is under attack. For deliberate attacks on the HSR-A hypernetwork, Node 391 with the highest comprehensive importance in the hypernetwork is selected for attack. This node corresponds to Beijing West Railway Station in the actual HSR network. It can be seen from the Figure 6 that the robustness critical threshold T_C of the HSR-A hypernetwork is 0.35 under random attacks, and 0.55 under deliberate attacks. Thus, the HSR-A hypernetwork is robust against random attacks and vulnerable to deliberate attacks.

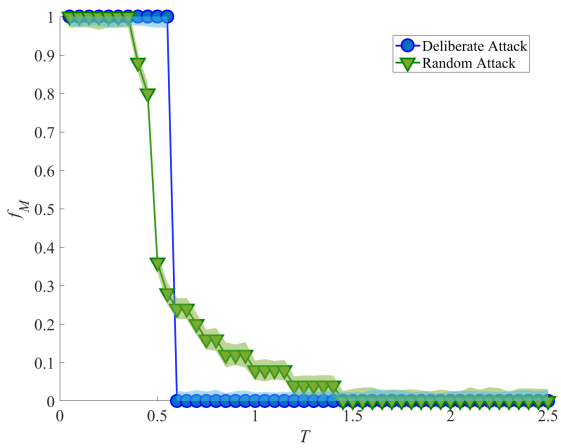


Figure 6. The hyperedge failure ratio f_M of the HSR-A hypernetwork under random attacks and deliberate attacks with different capacity parameters T.

Figure 7 shows the variation in the hyperedge failure ratio f_M with the capacity parameter T when the HSR-R hypernetwork is under attack. For deliberate attacks on the HSR-R hypernetwork, Node 114 with the highest comprehensive node importance is selected. This node corresponds to Chengdu East Railway Station in the actual HSR network. It can be seen from the figure that the critical threshold T_C of the HSR-R hypernetwork is 0.11 under random attacks and 0.45 under deliberate attacks. Since a smaller T_C indicates stronger hypernetwork robustness, the conclusion is that the HSR-R hypernetwork is robust against random attacks and vulnerable to deliberate attacks.

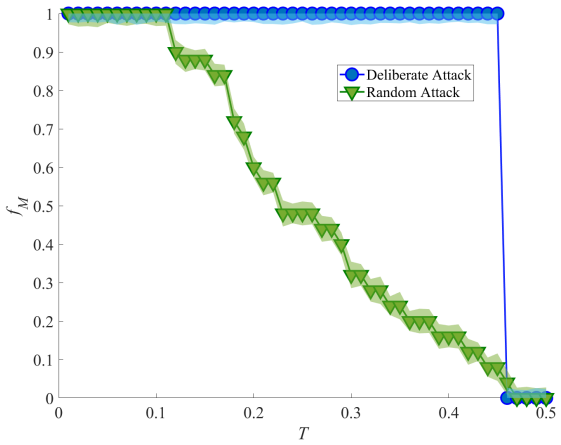


Figure 7. The hyperedge failure ratio f_M of the HSR-R hypernetwork under random attacks and deliberate attacks with different capacity parameters T.

Figure 8 shows the variation in the hyperedge failure ratio f_M with the capacity parameter T when the HSR-P hypernetwork is under attack. For deliberate attacks on the HSR-P hypernetwork, Node 53 with the highest comprehensive node importance is selected. This node corresponds to Xi'an North Railway Station in the actual HSR network. It can be seen from the figure that the critical threshold T_C of the HSR-P hypernetwork is 0.14 under random attacks and 0.53 under deliberate attacks. Similarly, since a smaller T_C indicates stronger hypernetwork robustness, the conclusion is that the HSR-P hypernetwork is robust against random attacks and vulnerable to deliberate attacks.

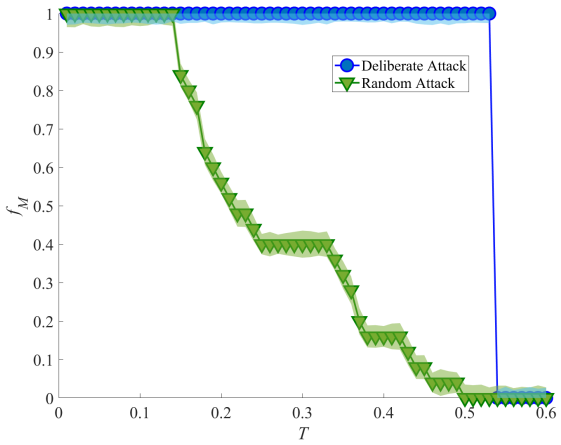


Figure 8. The hyperedge failure ratio f_M of the HSR-P hypernetwork under random attacks and deliberate attacks with different capacity parameters T.

Figure 9 shows the variation in the hyperedge failure ratio f_M with the capacity parameter T when the HSR-F hypernetwork is under attack. For deliberate attacks on the HSR-F hypernetwork, Node 391 with the highest comprehensive node importance is selected. This node corresponds to Beijing West Railway Station in the actual HSR network. It can be seen from the figure that the critical threshold T_C of the HSR-F hypernetwork is 0.08 under random attacks and 0.35 under deliberate attacks. Thus, the conclusion is that the HSR-F hypernetwork is robust against random attacks and vulnerable to deliberate attacks.

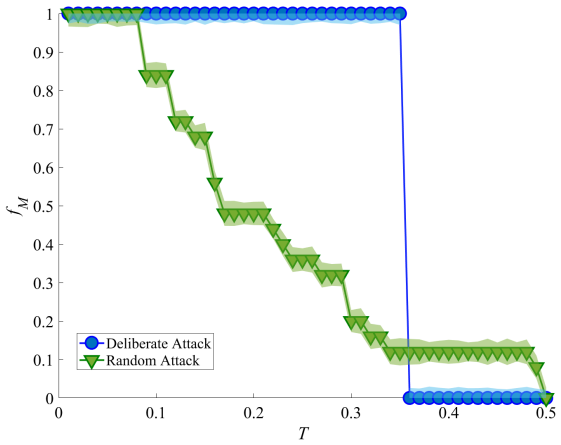


Figure 9. The hyperedge failure ratio f_M of the HSR-F hypernetwork under random attacks and deliberate attacks with different capacity parameters T.

Table 6 presents the specific robustness critical thresholds TC of the four HSR hypernetworks under attacks. Analysis of the data in Table 6 leads to the following conclusion: the robustness of the HSR hypernetworks against attacks ranks from best to worst as follows: HSR-F hypernetwork, HSR-R hypernetwork, HSR-P hypernetwork, and HSR-A hypernetwork. From a macro perspective, the total number of ordinary edges in each of the four HSR hypernetworks is as follows: 13722 for the HSR-F hypernetwork, 7063 for the HSR-R hypernetwork, 1438 for the HSR-P hypernetwork, and 1238 for the HSR-A hypernetwork. From a micro perspective, take the Shanghai-Kunming High-Speed Railway—the line with the most stations—as an example. Within the HSR-F hypernetwork, the number of ordinary edges in the Shanghai-Kunming HSR line is still the largest. This indicates that the more ordinary edges within hyperedges, the stronger the hypernetwork robustness. In other words, the more sub-lines within a HSR line, the more robust the HSR line becomes.

Table 6. Robustness Critical Thresholds T_C of the four HSR Hypernetworks.

HSR Hypernetwork Type	Random Attack	Deliberate Attack
HSR-A	0.35	0.55
HSR-P	0.14	0.53
HSR-R	0.11	0.45
HSR-F	0.08	0.35

5. Optimization Strategies

A conclusion is drawn from the robustness analysis in Section 4: the more sub-lines within a HSR line, the stronger the robustness of the HSR hypernetwork. Meanwhile, it can be clearly seen from Table 6 that the robustness of HSR hypernetworks under attacks is superior to that of the real-world hypernetwork, regardless of whether they adopt preferential attachment, random connection, or full connection. In the real world, with the continuous improvement of public security capacity, the probability of malicious incidents involving deliberate damage to HSR stations is extremely low. However, some uncertain events, such as natural disasters, pose a huge threat to the operation of the HSR system due to their high randomness. Thus, increasing the number of sub-lines within HSR lines can significantly improve the robustness of high-speed railways against random disturbances.

To more intuitively determine which internal hyperedge structure is more suitable for improving the robustness of HSR hypernetworks, the cost index $COST$ is presented below.

$$COST = \frac{reality_{T_C} - structure_{T_C}}{reality_{T_C}} \times \frac{structure_m - reality_m}{reality_m}, \quad (10)$$

where $reality_{T_C}$ denotes the robustness critical threshold of the real-world HSR hypernetwork. $structure_{T_C}$ denotes the robustness critical thresholds of the three hypernetworks based on internal hyperedge structures. $reality_m$ represents the number of sub-lines within hyperedges of the real-world HSR hypernetwork. $structure_m$ represents the number of sub-lines within hyperedges of the three hypernetworks based on internal hyperedge structures.

Table 7 presents the deployment costs of the three HSR hypernetworks based on internal hyperedge structures. Combining the data in Tables 6 and 7, it can be clearly seen that the HSR-F hypernetwork has the best robustness. However, this connection method is overly idealized. It requires pairwise connections between all stations within the same line, leading to high deployment costs for sub-lines within the line. Compared with the full connection method within hyperedges, the HSR-R hypernetwork saves a certain amount of cost. However, due to the randomness of sub-line deployment within its lines, there is a high probability that two HSR stations with low passenger flow within the line will form a sub-line. This results in the waste of sub-line resources. Thus, the preferential attachment method within hyperedges of HSR hypernetworks, that is the HSR-P hypernetwork, is the most feasible method for constructing sub-lines within lines. This is because the preferential attachment method within lines prioritizes sub-line deployment with hub nodes having the highest hyperdegree. This increases the robustness of the line, thereby improving the robustness of the entire HSR network.

Table 7. Optimization Costs of HSR Hypernetworks.

HSR Hypernetwork Type	Random Attack	Deliberate Attack
HSR-P	0.09	0.006
HSR-R	3.25	0.85
HSR-F	7.76	3.63

To further verify the conclusion that HSR-P is the optimal scenario and evaluate the feasibility of preferential attachment in practical applications, a sensitivity analysis is conducted, with results shown in Figure 10. The change in $COST$ is calculated by simulating variations in the δ_m parameter. As δ_m increases, the number of sub-lines rises, leading to a slight increase in cost. However, the $COST$ of HSR-P remains significantly lower than that of HSR-R and HSR-F. This indicates that in practical HSR planning, even with parameter fluctuations (i.e., changes in the number of hub-prioritized nodes), the preferential attachment mechanism can still balance robustness and economy, avoiding redundancy.

Although this cost index ($COST$) provides an effective framework for quantifying robustness and the economy of sub-line deployment, attention should be paid to the limitations of its assumptions. The formula only considers the relative changes in the number of sub-lines. Actual HSR construction costs vary significantly. They depend on multiple factors such as terrain along the line, station capacity, land acquisition costs, and engineering difficulty. These factors may result in actual costs being much higher than simplified estimates. Thus, $COST$ should serve as a theoretical reference. It should be used in conjunction with multi-dimensional economic evaluations in practical engineering planning. This avoids the risk of over-simplification.

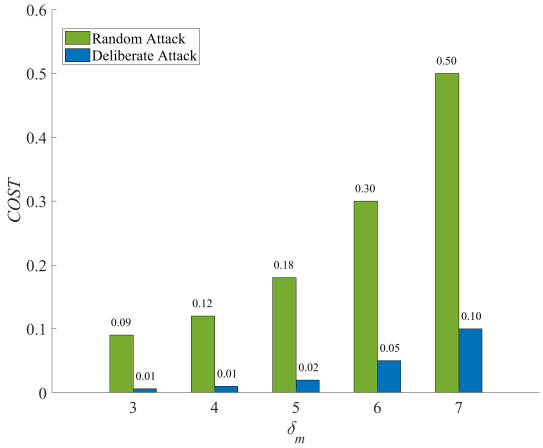


Figure 10. The Cost Sensitivity Analysis of the HSR-P Hypernetwork under Different δ_m.

6. Conclusions

To investigate the impact of internal hyperedge structures on the robustness of China's HSR hypernetworks, this study constructs a real-world HSR hypernetwork and three reconstructed hypernetworks based on hypernetwork theory. It combines the hypernetwork cascading failure model to analyze topological characteristics and robustness mechanisms, and balances robustness and economy through an optimization cost index. Research shows that the HSR-A hypernetwork, constructed by integrating HSR line and station data, has a node hyperdegree distribution conforming to a power law. It exhibits scale-free properties that are consistent with China's high-speed railway hub-and-spoke layout, providing a realistic foundation for robustness analysis. Comparative analysis of the four hypernetworks under random and deliberate attacks reveals that internal hyperedge structures significantly affect robustness: the HSR-F hypernetwork achieves the optimal robustness due to full connection of nodes within hyperedges, followed by the HSR-R and HSR-P hypernetworks, while the HSR-A hypernetwork has the weakest robustness as it only retains adjacent connections between stations. Further verification shows that the density of sub-lines within hyperedges is positively correlated with robustness. The denser the sub-lines, the more abundant the load redistribution paths when nodes fail, which can effectively suppress cascading failures. The optimization cost index defined in this study, which integrates robustness improvement and the number of sub-line deployments, shows the following: the HSR-F hypernetwork has the best robustness but requires full sub-line deployment within lines, resulting in excessively high costs; the HSR-R hypernetwork has lower costs but is prone to sub-line redundancy due to random connections; the HSR-P hypernetwork prioritizes sub-line deployment with hub stations, ensures good robustness while significantly reducing costs, and thus becomes the optimal solution balancing robustness and economy.

The improvement significance of the method proposed in this study for high-speed railway system design lies in the following aspects: By considering the internal structure of hyperedges, it provides a more realistic modeling framework. This framework can guide designers to prioritize the deployment of sub-lines around hub stations during the planning phase. This strategy not only improves network robustness but also quantifies economy by optimizing the cost index. In practical engineering planning, the optimized cost index can be used in conjunction with multi-dimensional economic evaluations. This avoids redundant investments. Furthermore, this method can also be extended to other transportation networks. It promotes the resilience improvement of the overall transportation system. Future work will focus on considering impacts such as recovery time and costs

under multi-node failure scenarios. These impacts will be integrated with the cascading failure model in this study to provide a more comprehensive optimization plan.

Author Contributions: B.Z. was responsible for the algorithm design, implementation, experiments, and manuscript writing. X.M. and F.M. supervised the research process and contributed to the manuscript revision and guidance. All authors have read and agreed to the published version of the manuscript.

Funding: This work was supported in part by the National Natural Science Foundation of China under Grant No. 62466049 and in part by the Science and Technology Plan of Qinghai Province under Grant No. 2025-ZJ-720.

Data Availability Statement: The datasets generated and analyzed during the current study are available from the first author, Bin Zhou, upon reasonable request.

Acknowledgments: The authors would like to thank the anonymous reviewers for their valuable comments and suggestions.

Conflicts of Interest: The authors declare no conflicts of interest.

Abbreviations

The following abbreviations are used in this manuscript:

HSR	High-Speed Railway
HSR-A	HSR hypernetwork with adjacent connections inside the hyperedges
HSR-R	HSR hypernetwork with random connections inside the hyperedges
HSR-P	HSR hypernetwork with preferential connections inside the hyperedges
HSR-F	HSR hypernetwork with full connections inside the hyperedges

References

1. National Railway Administration of the People's Republic of China. *2024 Railway Statistical Bulletin*; National Railway Administration of the People's Republic of China: Beijing, China, 2025.
2. Wang, C.; Meng, W.; Hou, X. The impact of high-speed rails on urban economy: An investigation using night lighting data of Chinese cities. *Res. Transp. Econ.* **2020**, *80*, 100819. [CrossRef]
3. Ye, C.; Zheng, Y.; Lin, S.; Zhao, Z. The Impact of High-Speed Railway Opening on Regional Economic Growth: The Case of the Wuhan-Guangzhou High-Speed Railway Line. *Sustainability* **2022**, *14*, 11390. [CrossRef]
4. Lordan, O.; Sallan, J.M. Analyzing the multilevel structure of the European airport network. *Chin. J. Aeronaut.* **2017**, *30*, 554–560. [CrossRef]
5. Du, W.B.; Zhou, X.L.; Lordan, O.; Wang, Z.; Zhao, C.; Zhu, Y.B. Analysis of the Chinese Airline Network as multi-layer networks. *Transp. Res. Part E Logist. Transp. Rev.* **2016**, *89*, 108–116. [CrossRef]
6. Zhang, J.H.; Hu, F.N.; Wang, S.L.; Dai, Y.; Wang, Y.X. Structural vulnerability and intervention of high speed railway networks. *Phys. A Stat. Mech. Its Appl.* **2016**, *462*, 743–751. [CrossRef]
7. Wandelt, S.; Shi, X.; Sun, X.Q. Estimation and improvement of transportation network robustness by exploiting communities. *Reliab. Eng. Syst. Saf.* **2021**, *206*, 107307. [CrossRef]
8. Li, T.; Rong, L.L. A comprehensive method for the robustness assessment of high-speed rail network with operation data: A case in China. *Transp. Res. Part A Policy Pract.* **2020**, *132*, 666–681. [CrossRef]
9. Mei, X.L.; Ye, W.J.; Li, W.J.; Chen, C.; Li, A.; Wu, J.P.; Du, H.B. Robustness Evaluation and Optimization of China's Multilayer Coupled Integrated Transportation System from a Complex Network Perspective. *Sustainability* **2025**, *17*, 7398. [CrossRef]
10. Huang, P.; Peng, Z.; Li, Z.; Peng, Q.Y. Solving the railway timetable rescheduling problem with graph neural networks. *Railw. Eng. Sci.* **2025**, 1–22. [CrossRef]
11. Tang, T.; Chai, S.M.; Wu, W.; Yin, J.T.; D'Ariano, A. A multi-task deep reinforcement learning approach to real-time railway train rescheduling. *Transp. Res. Part E Logist. Transp. Rev.* **2025**, *194*, 103900. [CrossRef]
12. Li, Z.C.; Huang, P.; Wen, C.; Dong, W.; Ji, Y.D.; Rodrigues, F. Railway network delay evolution: A heterogeneous graph neural network approach. *Appl. Soft Comput.* **2024**, *159*, 111640. [CrossRef]
13. Liu, X.W.; Chen, J.Q.; Du, B.; Yan, X.; Peng, Q.Y.; Shen, J. Resilience assessment of urban rail transit stations considering disturbance and time-varying passenger flow. *Comput.-Aided Civ. Infrastruct. Eng.* **2025**, *40*, 1627–1651. [CrossRef]

14. Xia, Y.Q.; Wang, K.W.; Tanirat, P.; Lee, B.; Moulitsas, I.; Li, J. Machine Learning driven complex network analysis of transport systems. *J. Transp. Geogr.* **2025**, *127*, 104270. [CrossRef]
15. Xu, J.Q.; Huang, H.N.; Pan, J.J.; Jiang, L.; Cheng, Y.Q. Identifying expressway network bottlenecks using iterative spectral bisection and OD detour degree. *Transp. A Transp. Sci.* **2025**, 1–37. [CrossRef]
16. Jiao, J.J.; Zhang, F.N.; Liu, J. A spatiotemporal analysis of the robustness of high-speed rail network in China. *Transp. Res. Part D Transp. Environ.* **2020**, *89*, 102584. [CrossRef]
17. Berge, C. *Graphs and hypergraphs*; North-Holland Pub. Co.: Amsterdam, The Netherlands, 1973.
18. Berge, C.; Sterboul, F. Equipartite colorings in graphs and hypergraphs. *J. Comb. Theory Ser. B* **1977**, *22*, 97–113. [CrossRef]
19. Hu, F.; Zhao, H.X.; He, J.B.; Li, F.X.; Li, S.L.; Zhang, Z.K. An evolving model for hypergraph-structure-based scientific collaboration networks. *Acta Phys. Sin.* **2013**, *62*, 198901.
20. Yu, W.; Sun, N. Establishment and Analysis of the Supernetwork Model for Nanjing Metro Transportation System. *Complexity* **2018**, *2018*, 4860531. [CrossRef]
21. Wang, J.; Ren, J.; Fu, X. Research on Bus and Metro Transfer From Perspective of Hypernetwork-A Case Study of Xi'an, China (December 2020). *IEEE Access* **2020**, *8*, 227048–227063. [CrossRef]
22. Luo, H.X.; Zhao, H.X.; Xiao, Y.Z.; Ye, Z.L.; Ma, H.Y.; Li, F.X. A Hypergraph-Based Analysis of the Topology and Robustness of Bus Hypernetworks. *J. Southwest Univ. Nat. Sci. Ed.* **2021**, *43*, 181–191.
23. Tang, K.; Xu, T.; Guo, T.Y.; Shao, F. Characteristics and robustness analysis of high-speed railway network in China: A hypernetwork perspective. *Syst. Eng.—Theory Pract.* **2024**, *44*, 3639–3649.
24. Yin, M.M.; Tang, K.; Xu, T.; Ding, J.H.; Guo, T.Y. Hypergraph-Based High-Speed Rail Hypernetwork Analysis and Node Importance Evaluation Using Operational Data: A Case Study of China. *J. Transp. Eng. Part A Syst.* **2025**, *152*, 04025113. [CrossRef]
25. Chen, Y.; Ma, X.J.; Ma, F.X.; Liu, Q.; Cheng, W.X. The Capacity Load Model of K-Uniform Hyper-Network based on Equal Load Distribution. *J. Phys. Conf. Ser.* **2021**, *1828*, 012060. [CrossRef]
26. Ma, W.X.; Lin, S.C.; Ci, Y.S.; Li, R.M. Resilience evaluation and improvement of post-disaster multimodal transportation networks. *Transp. Res. Part A Policy Pract.* **2024**, *189*, 104243. [CrossRef]
27. Motter, A.E.; Lai, Y.C. Cascade-based attacks on complex networks. *Phys. Rev. E* **2002**, *66*, 065102. [CrossRef]

Disclaimer/Publisher's Note: The statements, opinions and data contained in all publications are solely those of the individual author(s) and contributor(s) and not of MDPI and/or the editor(s). MDPI and/or the editor(s) disclaim responsibility for any injury to people or property resulting from any ideas, methods, instructions or products referred to in the content.